OPTICA ACTA, 1983, VOL. 30, NO. 1, 107–124

Regularized iterative and non-iterative procedures for object restoration from experimental data†

J. B. ABBISS‡, C. DE MOL§ and H. S. DHADWAL‡

(*Received 7 April 1982; revision received 8 June 1982*)

Abstract. A regularized algorithm for the recovery of band-limited signals from noisy data is described. The regularization is characterized by a single parameter. Iterative and non-iterative implementations of the algorithm are shown to have useful properties, the former offering the advantage of flexibility and the latter a potential for rapid data processing. Comparative results, using experimental data obtained in laser anemometry studies with a photon correlator, are presented both with and without regularization.

1. Introduction

The problem of inverting experimental data to derive explicit information concerning the structure of a source or scatterer has in recent years generated a vast literature [1, 2]. A specific problem which arises in Fourier optics consists in finding a solution to a Fredholm integral equation of the first kind, which has the general form

$$g(y)=\int_a^b K(x,y)f(x)\,dx, \tag{1}$$

where $g(y)$ is the measured image function (the image distribution) from which $f(x)$ (the object distribution) has to be determined. For a space-invariant system where the diffraction-limited coherent image is formed by a one-dimensional clear pupil extending over $(-\Omega,\Omega)$, the kernel takes the form

$$K(x,y)=\frac{\sin[\Omega(y-x)]}{\pi(y-x)} \tag{2}$$

and for an object lying between $-X$ and $+X$, the image field distribution becomes

$$g(y)=\int_{-X}^{X}\frac{\sin[\Omega(y-x)]}{\pi(y-x)}f(x)\,dx. \tag{3}$$

It is well known that attempts at inverting Fredholm integral equations of the first kind (for example, by matrix inversion), can, when the data are less than perfect, lead to highly erroneous results. Methods of imposing stability on the solution by the use of known or plausible constraints are available, however, and have been the subject of many studies [3]. A powerful iterative technique for solving these equations has also been proposed as a general solution to equation (1) by Landweber

† Some of the material contained in this paper formed part of a communication presented at the ICO-12 Meeting, Graz, Austria, 1981.

‡ Royal Aircraft Establishment, Farnborough, Hampshire, England.

§ Département de Mathématique, Université Libre de Bruxelles, Belgium.

[4], and in a form specifically for application to equation (3) by Gerchberg [5]. This procedure, now usually known as the Gerchberg method, has been shown to converge to the true solution in the absence of noise [6, 7]. It can be realized for computational purposes in a form which makes use of Fourier transforms alone, and can also be used to achieve explicit analytic continuation of a signal in a highly efficient manner. However, in its basic form the procedure is inherently unstable when the data are corrupted by noise or distorted in some other way. In this paper, therefore, we discuss methods for stabilizing the Gerchberg procedure and show how the computation can be reduced to a single operation on the original data set. We then demonstrate the performance of our algorithms by application to experimental data obtained in laser anemometry studies with a photon correlator.

Before describing the method in detail, we introduce the notation for the band-limiting and domain-limiting operators B_Ω and D_X:

$$B_\Omega[h(x)] = h(x) * \frac{\sin(\Omega x)}{\pi x}$$

$$= \int_{-\infty}^{\infty} \frac{\sin[\Omega(x-y)]}{\pi(x-y)} h(y)\, dy \tag{4}$$

and

$$D_X[h(x)] = \begin{cases} h(x), & |x| \leqslant X, \\ 0, & |x| > X, \end{cases} \tag{5}$$

where h belongs to the space $L^2(-\infty, \infty)$ of square-integrable functions. We denote the complement of D_X by $\bar{D}_X$:

$$\bar{D}_X[h(x)] = \begin{cases} 0, & |x| \leqslant X, \\ h(x), & |x| > X. \end{cases}$$

Thus, if I is the identity operator, $\bar{D}_X = I - D_X$. With the above notation, equation (3) becomes

$$g = B_\Omega D_X f. \tag{6}$$

Here we shall always be concerned with the class of objects for which $D_X f = f$. We denote Fourier transforms by the use of a circumflex:

$$\hat{h}(\omega) = \int_{-\infty}^{\infty} h(t) \exp(-i\omega t)\, \mathrm{d}t.$$

We also require certain simple rules for manipulating B_Ω and D_X:

$$\widehat{B_\Omega h} = D_\Omega \hat{h},$$
$$\widehat{D_X h} = B_X \hat{h},$$
$$\widehat{B_\Omega D_X h} = D_\Omega B_X \hat{h},$$
$$\widehat{D_X B_\Omega h} = B_X D_\Omega \hat{h}.$$

2. The iterative solution

The basis for the Gerchberg method [5] of solving equation (3) is that, since the object is of finite extent, the Fourier transform of the object field distribution is an entire function [8] and can be analytically continued [9, 10]. (The solution is also unique.) The actual procedure consists, at each iteration, of first truncating the latest estimate of the object to $(-X, X)$ and calculating its Fourier transform over the desired extrapolation length. The portion of this function in the range $(-\Omega, \Omega)$ is then replaced by the true spectrum over this range (that is, by the Fourier transform of the infinite image) and the resulting composite function is Fourier-transformed to form the new estimate. Thus, at the nth iteration the Fourier transform of the estimate of the object, say $\hat{f}_n$, is given by

$$\hat{f}_n = \tilde{g} + \bar{D}_\Omega(\widehat{D_X f_{n-1}}),$$

that is

$$\hat{f}_n = \hat{g} + \bar{D}_\Omega B_X \hat{f}_{n-1}. \tag{7}$$

(The process is begun by setting $\hat{f}_0$ equal to $\hat{g}$.) The nth estimate of the object is therefore

$$f_n = g + D_X f_{n-1} - B_\Omega D_X f_{n-1}$$

or

$$f_n = g + (I - B_\Omega) D_X f_{n-1}. \tag{8}$$

Numerous computer studies have demonstrated the performance of algorithms based on equation (7) for simulated data, and implementations of the method for various applications have been proposed [11–15].

2.1. *The regularized solution*

Up to this point, we have considered only operations involving ideal data, uncorrupted by noise or any other distorting factor. However, in the presence of perturbations to the data, the problem of inverting Fredholm integral equations of the first kind, such as equation (1), is ill-posed, in the sense that the solution does not depend continuously on the data, even if it is unique [3, 16]. Stability can be restored, and the effect of noise in the data controlled, by imposing on the solution a suitable constraint which may be derived from known or assumed object characteristics. This is the basis of the so-called regularization techniques of object and image restoration in optics [17, 18]. It should be noted that regularization involves essentially a modification of the original problem, which is transformed into one possessing the desired properties.

Let us denote the perturbations to the data (for example, the effects of noise) by the function r and rewrite equation (6) in the form

$$g = Af + r, \tag{9}$$

where

$$A = B_\Omega D_X. \tag{10}$$

A regularized solution, $\bar{f}$ say, can be derived in the following way [16, 18].

Suppose that ε is a measure in the root-mean-square sense of the quantity of noise in the image. We shall seek solutions f' which satisfy the inequality

$$\|g - Af'\| \leqslant \varepsilon, \tag{11}$$

where $\|\ \|$ denotes the L^2 norm:

$$\|g\|^2 = \int_{-\infty}^{\infty} |g(y)|^2\, dy.$$

The set of functions satisfying equation (11) is, however, unbounded, and in order to restrict the solution set still further we suppose that some *a priori* knowledge of f' is also available, expressible in the form

$$\|Cf'\| \leqslant E, \tag{12}$$

where C is a constraint operator and E is some positive number. If C is the identity operator, E represents an upper bound for the norm of f'. (In some physical applications, this constraint would appear naturally as an energy bound.)

The constraints (11) and (12) can be combined in the single inequality

$$\|g - Af'\|^2 + \left(\frac{\varepsilon}{E}\right)^2 \|Cf'\|^2 \leqslant 2\varepsilon^2. \tag{13}$$

Among the set of objects satisfying equation (13), a physically reasonable choice would be that object, $\tilde{f}$ say, which minimizes the left-hand side of the inequality. This solution satisfies the equation

$$\left[A^\dagger A + \left(\frac{\varepsilon}{E}\right)^2 C^\dagger C\right] \tilde{f} = A^\dagger g, \tag{14}$$

where the dagger denotes the adjoint operator. In our problem, A is the operator $B_\Omega D_\chi$ and it is not difficult to show that its adjoint is $D_\chi B_\Omega$. Hence equation (14) becomes

$$\left[D_\chi B_\Omega D_\chi + \left(\frac{\varepsilon}{E}\right)^2 C^\dagger C\right] \tilde{f} = D_\chi B_\Omega g,$$

since $B_\Omega^2 \equiv B_\Omega$.

As the simplest possible case, we take C to be the identity operator I, whence

$$\left[D_\chi B_\Omega D_\chi + \left(\frac{\varepsilon}{E}\right)^2 I\right] \tilde{f} = D_\chi B_\Omega g.$$

Since $D_\chi \tilde{f} = \tilde{f}$, this equation can also be written in the form

$$(D_\chi B_\Omega D_\chi + \alpha D_\chi)\tilde{f} = D_\chi B_\Omega g, \tag{15}$$

where $\alpha = (\varepsilon/E)^2$ is the so-called regularization parameter [3].

Further details of these techniques, together with extensive bibliographies of the subject, are available [3, 17, 19].

2.2. *Iterative methods for obtaining regularized solutions*

An iterative procedure which incorporates regularization, and reintroduces the original data set g at each step, can be derived in the following way. Equation (15) is first rewritten in the form

$$\tilde{f}=\tilde{f}+D_X B_\Omega g-(D_X B_\Omega D_X+\alpha D_X)\tilde{f}$$

or

$$\tilde{f}=D_X B_\Omega g+[(1-\alpha)D_X-D_X B_\Omega D_X]\tilde{f}. \tag{16}$$

This suggests that the regularized version of equation (8) might take the form

$$\tilde{f}_n=D_X B_\Omega g+[(1-\alpha)D_X-D_X B_\Omega D_X]\tilde{f}_{n-1}. \tag{17}$$

Fourier-transforming equation (17), and using the rules stated previously for the manipulation of the various operators, we obtain

$$\hat{\tilde{f}}_n=B_X[D_\Omega \hat{g}+(\bar{D}_\Omega-\alpha I)B_X\hat{\tilde{f}}_{n-1}].$$

Since the operator B_X outside the brackets in this expression is redundant for all intermediate steps, and will be needed only for the final estimate, the equation can be written as

$$\hat{\tilde{f}}_n=D_\Omega \hat{g}+(\bar{D}_\Omega-\alpha I)B_X\hat{\tilde{f}}_{n-1}. \tag{18}$$

By setting $\alpha=0$ the precise form of the Gerchberg algorithm in equation (7) is recovered, since from equation (6)

$$D_\Omega \hat{g}=\hat{g}$$

for noiseless data. However, for non-zero values of α the basic requirement of the Gerchberg method, that

$$D_\Omega \tilde{f}_n=D_\Omega \hat{g}$$

for all n, is not satisfied, since $\alpha B_X\hat{\tilde{f}}_{n-1}$ differs from zero over the range $(-\Omega,\Omega)$ of $\hat{g}$. Hence we seek to modify equation (15) appropriately.

Consider instead the regularization expressed by the equation

$$[(1-\alpha)D_X B_\Omega D_X+\alpha D_X]\tilde{f}=D_X B_\Omega g. \tag{19}$$

Rearranging as in equation (16), and setting $\lambda=1-\alpha$, we find that

$$\tilde{f}=D_X B_\Omega g+\lambda(D_X-D_X B_\Omega D_X)\tilde{f} \tag{20}$$

with the associated iteration formula

$$\tilde{f}_n=D_X B_\Omega g+\lambda(D_X-D_X B_\Omega D_X)\tilde{f}_{n-1}. \tag{21}$$

In conjugate space,

$$\hat{\tilde{f}}_n=B_X D_\Omega \hat{g}+\lambda(B_X-B_X D_\Omega B_X)\hat{\tilde{f}}_{n-1}$$

which, since $B_X=B_X^2$, can be written as

$$\hat{\tilde{f}}_n=B_X(D_\Omega \hat{g}+\lambda\bar{D}_\Omega B_X\hat{\tilde{f}}_{n-1}). \tag{22}$$

Using again the redundancy of the operator outside the brackets for all intermediate steps, we redefine the iterative procedure in the form

$$\hat{\bar{f}}_n = D_\Omega \hat{g} + \lambda \bar{D}_\Omega B_X \hat{\bar{f}}_{n-1}. \tag{23}$$

Each estimate is now identical with $D_\Omega \hat{g}$ over the range $(-\Omega, \Omega)$ and equation (7) is recovered by setting $\alpha = 0$ ($\lambda = 1$). Note that equation (22) will lead after n iterations to a band-limited approximation

$$\hat{\bar{f}}_n = B_X \hat{\bar{f}}_n,$$

whereas equation (23) will not. However, provided that they converge, both procedures will lead ultimately to the same function, $\hat{\bar{f}}_\infty$ say, which satisfies

$$\hat{\bar{f}}_\infty = B_X \hat{\bar{f}}_\infty,$$

so that the approximate solution given by equations (22) and (23) should not differ significantly when the number of iterations is high enough.

The convergence, for a given α, of equations (17) and (21) to the solutions of equations (15) and (19) respectively is guaranteed by the fact that the norms of the operators $(1-\alpha)D_X - D_X B_\Omega D_X$ and $\lambda(D_X - D_X B_\Omega D_X)$ are strictly bounded by unity if $\alpha < 1$. (If $0 < \alpha < \frac{1}{2}$, their norms are both $1-\alpha$.) This is easily established by using the well-known fact that the eigenvalues of $D_X B_\Omega D_X$ all lie between 0 and 1 [6, 18, 20].

On the other hand, it can be shown by using appropriate theorems in regularization theory that equations (15) and (19) define regularized solutions to equation (6); i.e. $\bar{f}$ will be close to the exact solution (if it exists) and will tend to it in some sense as the noise on the data g tends to zero. Although the proofs are too long to be given in detail here, the necessary results and theorems can be found, for instance, in the book by Groetsch [21].

We now demonstrate the way in which the iterative scheme embodied in equation (23) can be reduced to a single operation on the original data.

2.3. *The extrapolation matrix—a non-iterative regularized solution*

Both the regularized and unregularized iterative schemes embodied by equations (7) and (23) can easily be realized in a digital computer as a single matrix multiplication. Since

$$D_\Omega \hat{g} = D_\Omega \hat{\bar{f}}_{n-1}, \quad \forall n, \tag{24}$$

equation (23) can be rewritten as

$$\hat{\bar{f}}_n = (D_\Omega + \lambda \bar{D}_\Omega B_X) \hat{\bar{f}}_{n-1}.$$

Hence

$$\hat{\bar{f}}_n = (D_\Omega + \lambda \bar{D}_\Omega B_X)^n D_\Omega \hat{g}, \tag{25}$$

where we have taken $\hat{\bar{f}}_0 = D_\Omega \hat{g}$.

A related non-iterative but unregularized algorithm has been derived [11, 22, 23], which requires, however, either the inversion of the matrix approximating the operator $(I - \bar{D}_\Omega B_X)$ or, equivalently, the summation of a power series in $\bar{D}_\Omega B_X$.

We also remark at this point that other regularized iterative schemes can be constructed, which can again be implemented non-iteratively. For example, equation (15) can be rewritten in the form

$$(1+\alpha)D_X\tilde{f}=D_XB_\Omega g+(D_X-D_XB_\Omega D_X)\tilde{f},$$

leading to the iterative scheme, in the conjugate space,

$$\hat{\tilde{f}}_n=\frac{1}{1+\alpha}(D_\Omega\hat{g}+\bar{D}_\Omega B_X\hat{\tilde{f}}_{n-1}).$$

Because of the slight difference in the numerical factors, which are in the ratio $1/(1-\alpha^2)$, the final estimate generated by this scheme will differ very slightly from that of equation (23).

It should also be noted that if the index n in equation (25) is a power of 2, say 2^m, the number of matrix multiplications involved in raising $D_\Omega+\lambda\bar{D}_\Omega B_X$ to the power n can be reduced from $(n-1)$ to m, with a significant reduction in computational time.

Any practical computation based on equation (23) or (25) must involve a finite extrapolation from Ω to, say, Z. If D_Z denotes the related domain-limiting operator, the appropriate algorithms for practical applications then take the forms

$$\hat{\tilde{f}}_n=D_\Omega\hat{g}+\lambda D_Z\bar{D}_\Omega B_X\hat{\tilde{f}}_{n-1} \tag{26}$$

and

$$\hat{\tilde{f}}_n=(D_\Omega+\lambda D_Z\bar{D}_\Omega B_X)^nD_\Omega\hat{g}. \tag{27}$$

The estimates obtained from equations (26) and (27) will in fact converge not to $\tilde{f}$ but to a smoother solution, the resolution in which will depend on the value of Z.

3. Applications to laser anemometry data obtained with a photon correlator

During the past decade, laser anemometry has been intensively developed as a research tool in experimental fluid dynamics. In the most common arrangement the primary optical signal consists of the light scattered out of a pair of intersecting laser beams by small particles borne along with the flow. The Doppler shift in the frequency of this light is proportional to a component of the scattering particle's velocity; the direction of this component depends on the precise geometry of the arrangement. In applications where this scattered light is extremely weak—for example, in studies of high-speed flows over relatively long optical paths—data acquisition and processing may have to be carried out by photon-counting detectors and digital correlators operating in parallel with signal reception [24]. However, these instruments, which may be required to operate at sample times of 10 ns or less, are expensive to construct, and the number of output channels is usually restricted to 100 or so. Such a restriction can subsequently pose problems in the extraction from the data record of the required information concerning flow velocity.

This information may consist, if the signal is sufficiently strong, of a single velocity estimate corresponding to each transit of the measurement region by a scattering particle, or an estimate of the probability density function of the velocity if the autocorrelation function has been integrated over many particle transits. In either case, the velocity information can be extracted from the autocorrelation function by means of a Fourier transform [25]. We now show how, by exploiting

such a relationship, the resolution problem takes the same mathematical form as the optical example discussed above. We then make use of both the iterative and non-iterative procedures to achieve super-resolution of photon-correlation data.

We suppose that there is some upper limit, say u_m, to the support of the velocity distribution function $p(u)$. After some initial processing [25], the autocorrelation function $G(\tau)$ is related to $p(u)$ by a Fourier cosine transform:

$$G(\tau)=\int_0^{u_m} p(u)\cos(2\pi u\tau)\,du. \tag{28}$$

Note that if negative as well as positive values of u contribute to the data, only $p(|u|)$ is recoverable from equation (28); where necessary, however, appropriate experimental arrangements can be made to ensure that the effective contributions are always positive [25]. By using the Wiener–Khinchine theorem, equation (28) can be inverted to give

$$p(u)=4\int_0^{\infty} G(\tau)\cos(2\pi u\tau)\,d\tau. \tag{29}$$

In practice $G(\tau)$ is known only over $(0, \tau_m)$. Therefore the image of $p(u)$ is a blurred one, $q(u)$, say:

$$\begin{aligned} q(u)&=4\int_0^{\tau_m} G(\tau)\cos(2\pi u\tau)\,d\tau \\ &=4\int_0^{\tau_m}\cos(2\pi u\tau)\,d\tau\int_0^{u_m} p(v)\cos(2\pi v\tau)\,dv. \end{aligned}$$

If we make $p(u)$ an even function by letting $p(-u)=p(u)$, and also use the fact that $G(\tau)=G(-\tau)$, we can reduce the above equation to the form

$$q(u)=\int_{-u_m}^{u_m}\frac{\sin[2\pi\tau_m(u-v)]}{\pi(u-v)}p(v)\,dv. \tag{30}$$

Since equation (30) is mathematically equivalent to the imaging problem of equation (3), the iterative and non-iterative regularized algorithms of equations (26) and (27) can be directly applied to laser anemometry data obtained by photon-correlation techniques.

If a lower limit u_l for the support of the velocity distribution is also known *a priori*, equation (30) becomes

$$q(u)=2\int_{u_l}^{u_m}\frac{\sin[2\pi\tau_m(u-v)]}{\pi(u-v)}p(v)\,dv. \tag{31}$$

The definition of the operator D_X is modified appropriately, with the object now lying within the range

$$X_1\leqslant|x|\leqslant X_2.$$

The data used in the computer experiments were obtained during a study of the interaction between a shock-wave and a turbulent boundary layer [26], using a 64-channel correlator. Figure 1 shows the autocorrelation function, after initial processing, derived from a part of the flow which was known to be close to a shock wave. Because of the fluctuations in the location of the interaction, the position of the

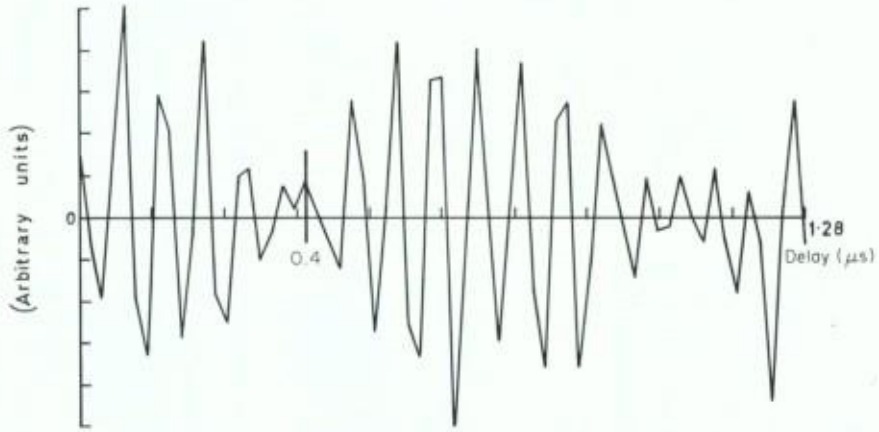

Figure 1. Autocorrelation function near a shock wave.

Figure 2. Fourier cosine transform of data of figure 1; peaks at 12·80 and 14·23 MHz.

shock-wave structure varied while the data were being acquired over a small streamwise distance, which included the measurement region. The data thus represent a time- and space-averaged velocity distribution, including subsonic and supersonic components, although turbulence levels were expected to be low in this part of the flow. The Fourier cosine transform of the data (figure 2) shows these characteristics clearly. The peaks corresponding to the subsonic and supersonic flow regions occur at 12·80 and 14·23 MHz. (Velocity can be calculated from Doppler frequency by means of known calibration constants.)

To illustrate the performance of the non-iterative extrapolation matrix algorithm based on equation (27), the record of figure 1 was truncated to include the first 21 data points only; the maximum value of τ is now 0·4 μs. The Fourier transform of this shortened record is given in figure 3; note that the separate peaks of figure 2 are no longer distinguishable.

As *a priori* information in the calculation of the analytically continued record, the true distribution was assumed to lie between the frequency limits defined by the first zero-crossings on either side of the central peak in figure 3. These limits are used to define the operator B_χ of equation (27), while the operator D_Ω is defined by the length

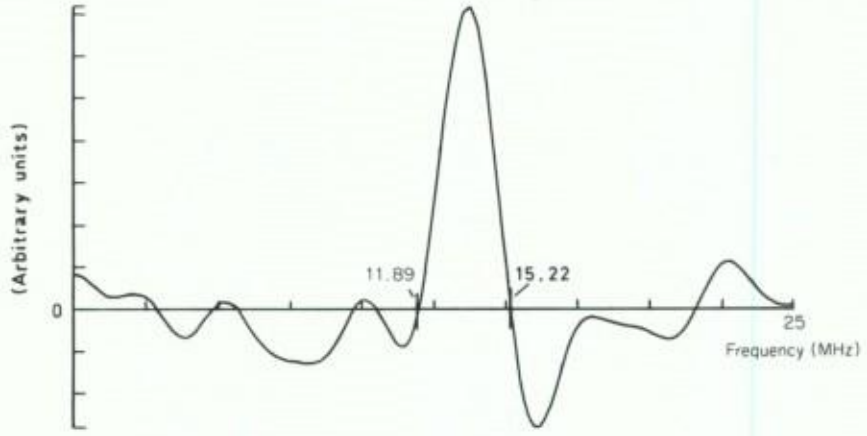

Figure 3. Fourier cosine transform of shortened data record ($\tau = 0{\cdot}0$–$0{\cdot}4\,\mu$s).

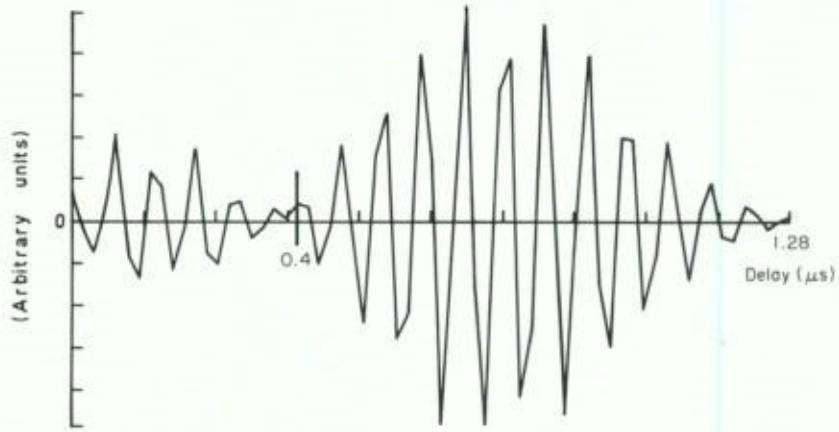

Figure 4. Shortened data record extrapolated from $\tau = 0{\cdot}4\,\mu$s to $\tau = 1{\cdot}28\,\mu$s using equation (27). Unregularized: $\lambda = 1$. (2^{10} iterations.)

of the shortened record. (Note that if the limits assigned to the distribution are too narrowly set, some distortion will inevitably result.) The non-regularized matrix ($\lambda = 1$) was computed for extrapolation from the initial 21 data points to the 65 data points of the original record, and for 2^{10} (1024) iterations; figure 4 shows the extrapolated function. It is evident that the maximum excursions in the extrapolated part are significantly greater than those of the basic data set. With further iteration this imbalance increases.

In figure 5 this unstable behaviour has been controlled (for the same extrapolation length) by introducing regularization, the parameter λ having the value of 0·993. In the Fourier transform plane (figure 6), the single peak is now clearly resolved into the expected two components. Closer examination reveals that the peak positions are at 12·88 and 14·30 MHz; thus the errors in location, compared with figure 2, are about 0·5 per cent. Further iteration, as far as 2^{20} (over 10^6), introduces no signs of instability. At 2^9 iterations the object amplitude distribution has in fact already converged to within 0·5 per cent of its final state.

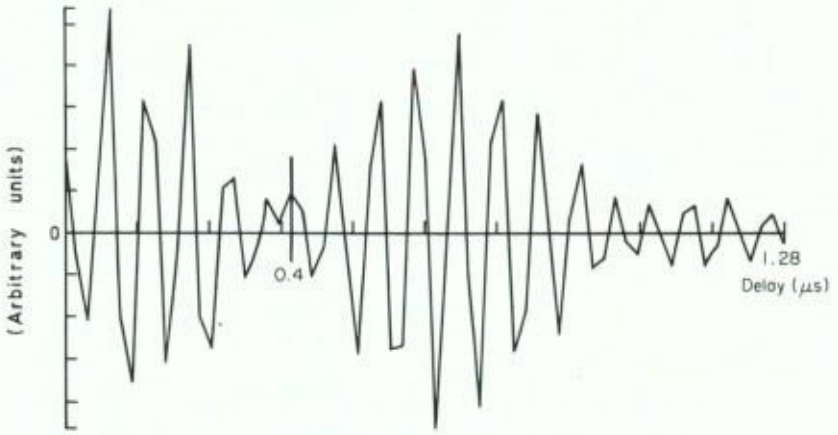

Figure 5. Extrapolation as for figure 4. Regularized: $\lambda = 0{\cdot}993$.

Figure 6. Object estimate corresponding to figure 5: peaks at 12·88 and 14·30 MHz.

For this degree of extrapolation, no advantage is found by using smaller values of λ; the effect is simply to reduce the degree of resolution in the Fourier transform plane. Controlled extrapolation to greater record lengths can be achieved with a smaller λ, but the final result is very similar to figure 6. The optimal value for λ will depend on the criteria used to assess the final estimate, as well as on the properties of the original data. This problem has been discussed by several authors (see, for example, [3, 27]) and is under investigation for the particular application considered here.

It should be remarked here that the large excursions in the data at the end of the experimental record of figure 1 arise from noise on the signal, which is amplified by the preprocessing technique used. These features do not appear in the extrapolated functions shown in figures 4 and 5; their absence is attributable to the smoothing properties of the band-limiting operators involved. On the other hand, distortions of the data occurring at very small values of τ (which originate in the detector) are preserved as part of the basic data set. Since both backward and forward extrapolation are possible with the procedures considered in this paper, these distortions could also be reduced by appropriate minor modifications of the algorithms.

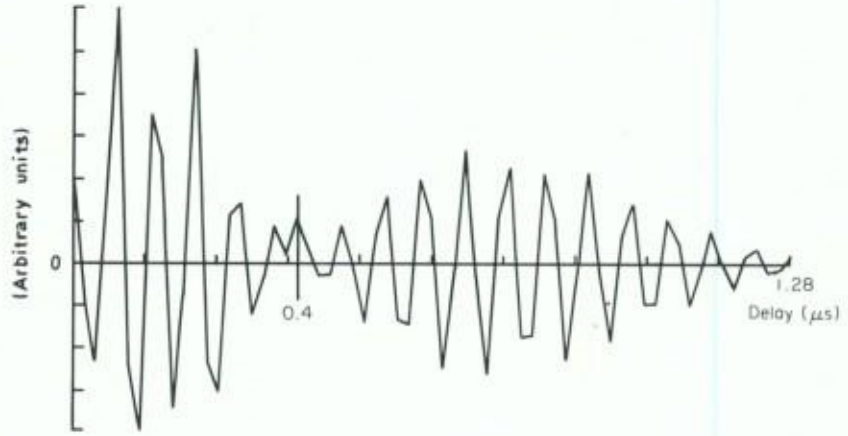

Figure 7. Data extrapolated from $\tau = 0{\cdot}4\,\mu s$ to $\tau = 1{\cdot}28\,\mu s$ using equation (26). Positivity constraint only ($\lambda = 1$); 2^{10} iterations.

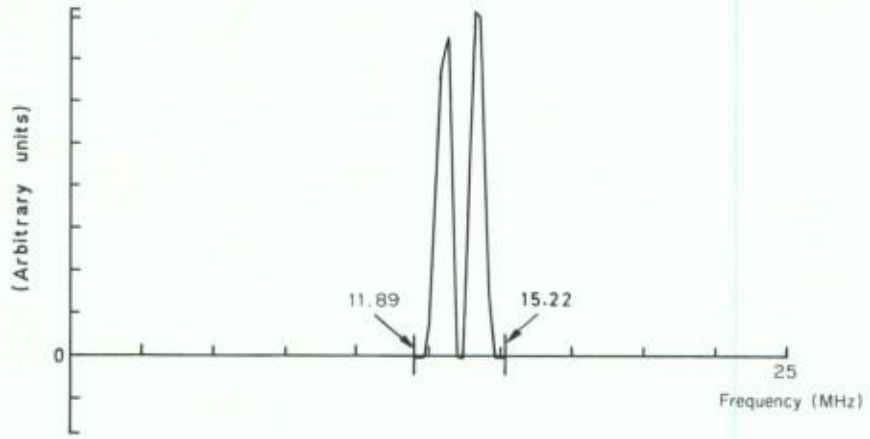

Figure 8. Object estimate corresponding to figure 7.

A disadvantage of the non-iterative method embodied in equation (27) is the apparent impossibility of incorporating the powerful additional constraint of positivity, when this is known to be a characteristic of the object function. Since this is certainly the case for the velocity probability density distributions considered above, the effect of incorporating positivity in the calculations has been explored with the aid of the iterative formula of equation (26). Starting with the same shortened experimental record, it was first confirmed that with and without positivity the same results were obtained as before, for various values of the regularization parameter λ and the same extrapolation factor. However, application of the positivity constraint alone was now sufficient to suppress the instability previously encountered for $\lambda = 1$ (see figure 4). The extrapolated function and the corresponding object are shown in figures 7 and 8. In fact, the requirement that the object be positive, when combined with the blurring of formula (27), can be viewed as a form of regularization [28].

We now consider the application of the iterative procedure of equation (26) to improving the estimation of the variance of a narrow distribution in the Fourier

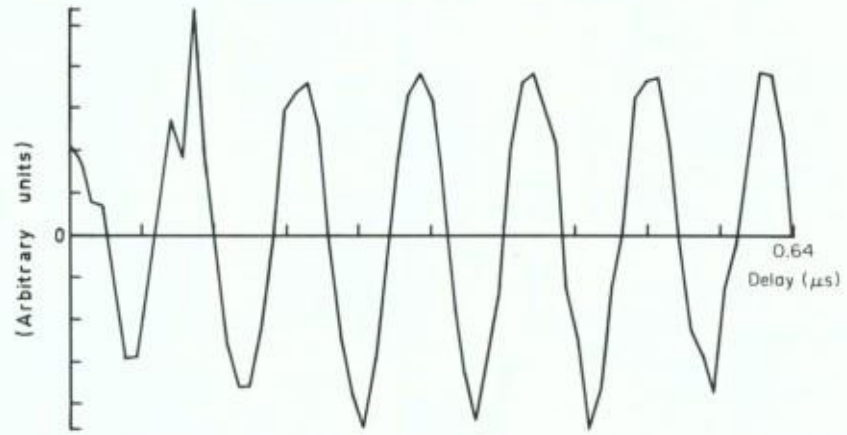

Figure 9. Autocorrelation function at a point upstream of interaction region.

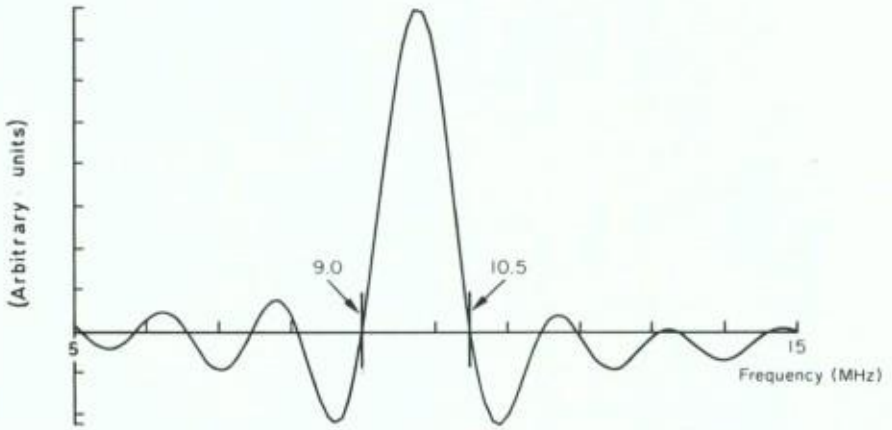

Figure 10. Fourier cosine transform of data of figure 9. Apparent turbulence intensity = 3·4 per cent.

transform plane. The experimental data, shown in figure 9, are again taken from the laser anemometry studies described above. In this case the measurement was made upstream of the interaction features at a point in the test section where the flow velocity was supersonic and low turbulence levels were expected. Turbulence intensity is defined as the ratio of the standard deviation of the velocity distribution to the mean; an accurate estimation of the standard deviation is thus of fundamental importance in the determination of low turbulence intensity.

Figure 10 is the distribution obtained by Fourier-transforming the data of figure 9. The width of this distribution is predominantly due to the truncation of the experimental data, and the apparent turbulence intensity (about 3·4 per cent) is well above the expected value in this part of the flow. For a purely cosinusoidal record (that is, for laminar flow) this apparent turbulence intensity, ψ say, would be due entirely to truncation broadening, and in fact can be calculated exactly. If the record contains γ cycles, where γ is not necessarily an integer, it can be shown [29] that

$$\psi = \frac{1}{k\gamma},$$

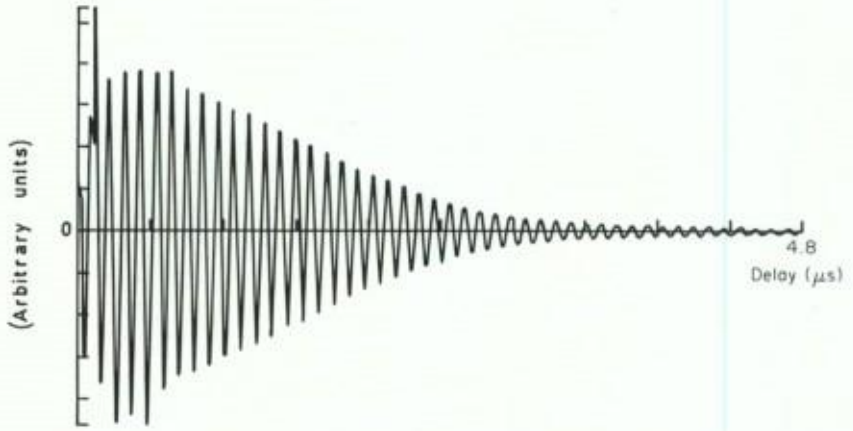

Figure 11. Data of figure 9 extrapolated to $\tau = 4{\cdot}8\,\mu s$ using equation (26). Positivity constraint only ($\lambda = 1$); 2^{10} iterations.

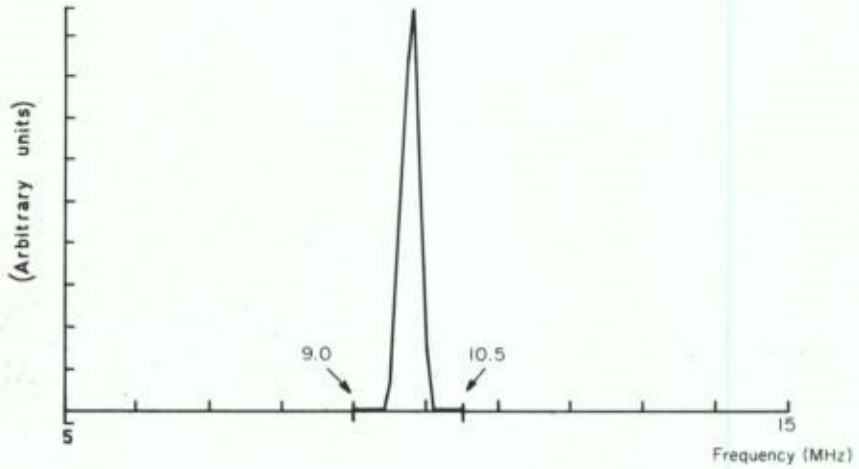

Figure 12. Object estimate corresponding to figure 11. Apparent turbulence intensity = 1·25 per cent.

where

$$k^2 = 2\pi \int_{-\pi}^{\pi} \frac{\sin x}{x}\, dx;$$

From tables, $k \simeq 4{\cdot}82$. For figure 9, ψ is found to have the value of 0·033 (3·3 per cent). In order to extract a better estimate of the turbulence level, the data of figure 9 were analytically continued, using equation (26) and applying the positivity constraint only (λ being set equal to 1), from an initial maximum of $\tau = 0{\cdot}64\,\mu s$ to values which progressively reduced the effect of broadening due to truncation. The band limits for the extrapolation were again taken to be the first zero-crossings on either side of the peak. Figures 11 and 12 show the extrapolated function and the object estimate, obtained after 1024 iterations, for extrapolation by a factor of 7·5 (the maximum attempted); both functions remain well behaved. The inclusion of the positivity constraint had little effect on the behaviour of the function at small extrapolation lengths when compared with extrapolation without positivity ($\lambda = 1$ for all cases). For

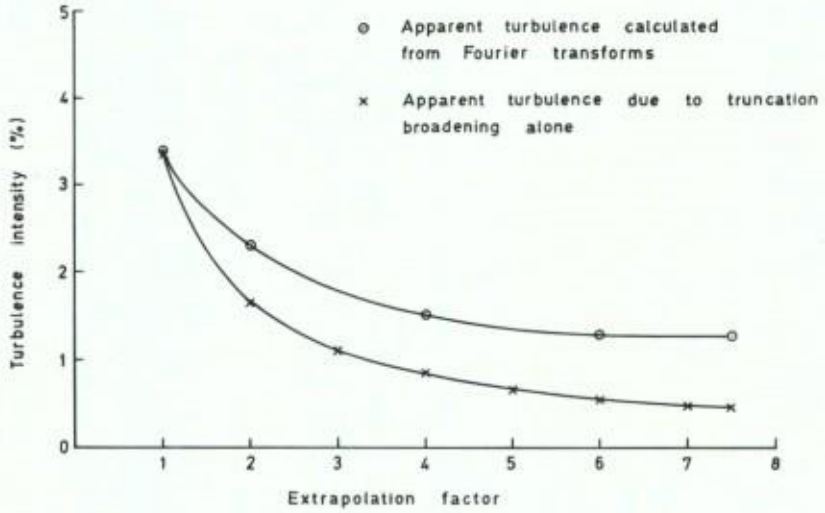

Figure 13. Apparent turbulance against extrapolation factor.

greater lengths, however, positivity alone was found to be sufficient to provide adequate control of the extrapolation process. In figure 13 the apparent turbulence intensity computed from the Fourier transform of the extrapolated function is plotted for several different extrapolation factors. From this curve it would appear that the 'true' turbulence intensity is about 1·25 per cent. (Genuine turbulence in this part of the flow is probably well below this level. Acoustic disturbances originating in the upstream boundary layer could, however, be expected to contribute fluctuations of about 1 per cent (K. G. Winter 1982, private communication).)

4. Discussion

In recent years the Gerchberg algorithm has been the subject of considerable interest, and despite an underlying instability its performance in the presence of noise has often proved more controlled than might be expected from, for example, arguments based on an eigenfunction analysis of equation (3) [7, 20, 30]. Some effort has also been directed towards improving the rate of convergence of the basic algorithm [31, 32]. However, if the method is to be generally applicable, some form of regularization is clearly necessary; to the best of our knowledge the modifications described here, developed initially for use in photon correlation anemometry, have not been previously proposed. The regularized scheme of Cesini *et al.* [33], which is also based on an iterative filtering technique, uses a different operator for the generation of successive estimates. They demonstrate that, in the limit, their procedure is equivalent to Wiener filtering. Other classes of regularized iterative scheme have been proposed for more general Fredholm integral equations of the first kind [27, 34].

The increase in resolution for the low-turbulence example of figures 9 to 13, as measured by the ratio of the standard deviations of the initial and final velocity distributions, is about 2·7, the maximum extrapolation factor being 7·5. By analysing the Gerchberg procedure with the aid of the prolate spheroidal wavefunctions (the eigenfunctions of the low-pass filter of equation (3)), De Santis and Gori [7] have established that in the absence of noise the computational effort involved in

extrapolating band-limited signals depends directly on the time-bandwidth (or space-bandwidth) product c corresponding to the original measurement. They showed that increasing the number of iterations is equivalent to increasing the resolution; the lower the value of c, the smaller the number of iterations required for a given increase in resolution. For the photon correlation data described above, and with the definition used by De Santis and Gori [7] ($c=4u_m\tau_m$ in our notation), the time-bandwidth product has the values 24·4 for figure 3 and 26·9 for figure 10. In assessing the results presented here, however, account should also be taken of the non-zero lower limits assumed for the velocity distribution support; thus, for the band-pass filter of equation (31), the appropriate time-bandwidth product c' is defined by

$$c'=4(u_m-u_l)\tau_m.$$

Although the complete numerical behaviour of the eigenvalues for the band-pass kernel has not been explicitly determined, investigations by Landau [35] suggest that in this case the significant number of eigenvalues is approximately c'; for figures 3 and 10, c' has the values 5·3 and 3·8 respectively. Bertero and Pike [36] have shown in the case of the low-pass filter (equation (3)) that, as c falls below about 5, the degree of super-resolution attainable begins to rise rapidly, the predicted values depending of course on the ratio of signal to noise in the data. It would seem that data obtained in photon correlation laser anemometry experiments on flows characterized by narrow velocity distributions may be particularly suitable for the application of procedures designed to achieve super-resolution.

It should be remarked that the theory presented here is based on the properties of continuous functions, whereas the data to which the results have been applied consist of discrete measurements. For both sets of data (figures 1 and 9) these measurements were made at well above the Nyquist rate. The question of the precise relationship between the sampling rate and the characteristics of the reconstructed object is still under investigation.

5. Conclusions

In this paper we have concentrated on the application of the algorithms to one-dimensional signals, but the procedures could, in principle, be extended to two-dimensional object restoration problems. Implementation in two dimensions would also be possible in a simple and very efficient manner with passive optical components. The regularization parameter λ could be incorporated in Marks' scheme [13], for example, by the addition of a neutral density filter at the input mirror.

Experimental data obtained from laser anemometry studies of a transonic airflow have been used to demonstrate the performance of regularized algorithms based on the Gerchberg iterative procedure for achieving analytic continuation of band-limited signals, and it has been shown that the effects of noise in the data can be controlled by a suitable choice of the regularization parameter. The imposition of a positivity constraint on the object estimate was found, for one type of object at least, to have an effect similar to that of regularization. The non-iterative method of equation (27) has been found to be capable of conferring an advantage in speed of processing over the iterative procedure of equation (26). The iterative technique is, however, more flexible and makes possible the incorporation of other constraints, such as positivity or variable band limits.

Acknowledgments

C. De Mol is Chercheur qualifié du Fonds National Belge de la Recherche Scientifique, and Visiting Fellow at Queen Elizabeth College, University of London, under the terms of a contract with the U.K. Ministry of Defence; the financial support provided by this contract is gratefully acknowledged. We also wish to thank members of staff of the Physics Department at Queen Elizabeth College for stimulating discussions, and Dr. M. Bertero of the University of Genoa, Italy, for valuable help in clarifying certain ideas contained in this work. We are also grateful to Dr. F. Gori of the University of Rome for a helpful comment on the manuscript, and to Dr. Bertero and Dr. E. R. Pike of the Royal Signals and Radar Establishment, Ministry of Defence, for making available to us a preprint of a forthcoming publication.

On décrit un algorithme régularisé pour la restitution de signaux à bande limitée à partir de données bruitées. La régularisation est caractérisée par un seul paramètre. On montre que des utilisations itératives et non itératives de l'algorithme ont des propriétés utiles, d'abord en offrant l'avantage de la flexibilité et ensuite pour la possibilité de traitement de donnéesrapide. Des résultats comparatifs, utilisant des données expérimentales obtenues dans des études de vélocimétrie laser avec un corrélateur de photons, sont présentés à la fois avec et sans régularisation.

Es wird ein regularisierter Algorithmus für die Rückgewinnung von bandbegrenzten Signalen aus verrauschten Signalen beschrieben. Die Regularisierung wird durch einen einzigen Parameter charakterisiert. Iterative und nichtiterative Versionen des Algorithmus haben nützliche Eigenschaften gezeigt, wobei die ersteren den Vorteil der Flexiblität und die letzteren die Möglichkeit schneller Datenverarbeitung bieten. Vergleichbare Ergebnisse, sowohl mit als auch ohne Regularisierung werden präsentiert, wobei experimentelle Daten aus Laser-Anemometrie-Studien mit einem Photonenkorrelator benutzt werden.

References

[1] Baltes, H. P. (editor), 1978, *Inverse Source Problems in Optics*, Topics in Current Physics, Vol. 9 (Berlin, Heidelberg, New York: Springer-Verlag).
[2] Baltes, H. P. (editor), 1980, *Inverse Scattering Problems in Optics*, Topics in Current Physics, Vol. 20 (Berlin, Heidelberg, New York: Springer-Verlag).
[3] Tikhonov, A. N., and Arsenin, V. Y., 1977, *Solutions of Ill-posed Problems* (Washington, D.C.: V. H. Winston & Sons).
[4] Landweber, L., 1951, *Am. J. Math.*, **73,** 615.
[5] Gerchberg, R. W., 1974, *Optica Acta*, **21,** 709.
[6] Papoulis, A., 1975, *I.E.E.E. Trans. Circuits Systems*, **22,** 735.
[7] De Santis, P., and Gori, F., 1975, *Optica Acta*, **22,** 691.
[8] Boas, R. P., 1954, *Entire Functions* (New York, London: Academic Press).
[9] Wolter, H., 1961, *Progress in Optics*, Vol. 1, edited by E. Wolf (Amsterdam: North-Holland), p. 157.
[10] Frieden, B. R., 1971, *Progress in Optics*, Vol. 9, edited by E. Wolf (Amsterdam: North-Holland), p. 313.
[11] Sabri, M. S., and Steenaart, W., 1978, *I.E.E.E. Trans. Circuits Systems*, **25,** 74.
[12] Papoulis, A., and Chamzas, C., 1979, *Ultrasonic Imaging*, **1,** 121.
[13] Marks, R. J., II, 1980, *Appl. Optics*, **19,** 1670.
[14] Marks, R. J., II, 1981, *Appl. Optics*, **20,** 1815.
[15] Sato, T., Norton, S. J., Linzer, M., Ikeda, O., and Hirama, M., 1981, *Appl. Optics*, **20,** 395.
[16] Miller, K., 1970, *SIAM J. math. Analysis*, **1,** 52.

[17] BERTERO, M., DE MOL, C., and VIANO, G. A., 1980, *Inverse Scattering Problems in Optics*, edited by H. P. Baltes, Topics in Current Physics, Vol. 20 (Berlin, Heidelberg, New York: Springer-Verlag), p. 161.
[18] BERTERO, M., VIANO, G. A., and DE MOL, C., 1980, *Optica Acta*, **27**, 307.
[19] NASHED, M. Z., 1981, *I.E.E.E. Trans. Antennas Propag.*, **29**, 220.
[20] SLEPIAN, D., and POLLAK, H. O., 1961, *Bell Syst. tech. J.*, **40**, 43.
[21] GROETSCH, C. W., 1977, *Generalized Inverses of Linear Operators* (*New York, Basle, Marcel Dekker, Inc*).
[22] CADZOW, J. A., 1979, *I.E.E.E. Trans. Acoust. Speech Signal Process.*, **27**, 4.
[23] SABRI, M. S., and STEENAART, W., 1980, *I.E.E.E. Trans. Acoust. Speech Signal Process.*, **28**, 254.
[24] CUMMINS, H. Z., and PIKE, E. R. (editors), 1974, *Photon Correlation and Light Beating Spectroscopy* (New York: Plenum Press).
[25] ABBISS, J. B., 1977, *Photon Correlation Spectroscopy and Velocimetry*, edited by H. Z. Cummins and E. R. Pike (New York: Plenum Press), p. 386.
[26] ABBISS, J. B., DHADWAL, H. S., SHARPE, P. R., and WRIGHT, M. P., 1981, *Proceedings, ICIASF* '81 (New York: IEEE).
[27] MILLER, G. F., 1974, *Numerical Solution of Integral Equations*, edited by L. M. Delves and J. Walsh (Oxford University Press), p. 175.
[28] BERTERO, M., and DOVI, V., 1981, *Optica Acta*, **28**, 1635.
[29] ABBISS, J. B., 1979, *Physica Scripta*, **19**, 388.
[30] RUSHFORTH, C. K., and FROST, R. L., 1980, *J. opt. Soc. Am.*, **70**, 1539.
[31] CAHANA, D., and STARK, H., 1981, *Appl. Optics*, **20**, 2780.
[32] MAITRE, H., 1981, *Optica Acta*, **28**, 973.
[33] CESINI, G., GUATTARI, G., LUCARINI, G., and PALMA, C., 1978, *Optica Acta*, **25**, 501.
[34] STRAND, O. N., 1974, *SIAM J. num. Analysis*, **11**, 798.
[35] LANDAU, H. J., 1965, *Trans. Am. math. Soc.*, **115**, 242.
[36] BERTERO, M., and PIKE, E. R., 1982, *Optica Acta*, **29**, 727.